

**LNF-97/047**

# **Temperature Dependence of Non-Debye Disorder in Doped Manganites**

C. Meneghini, R. Cimino, S. Pascarelli, S. Mobilio, C. Raghu, D.D. Sarma

*Physical Review B* 56, 7, 3520–3523, (1997)

## Temperature dependence of non-Debye disorder in doped manganites

C. Meneghini

*Laboratori Nazionali di Frascati, INFN, P.O. Box 13, I-00044 Frascati, Italy  
and Istituto Nazionale di Fisica della Materia (INFN), Via dell'Acciaio 139, I-16153 Genova, Italy*

R. Cimino

*Laboratori Nazionali di Frascati, INFN, P.O. Box 13, I-00044 Frascati, Italy*

S. Pascarelli

*Istituto Nazionale di Fisica della Materia (INFN), via dell'Acciaio 139, I-16153 Genova, Italy*

S. Mobilio

*Laboratori Nazionali di Frascati, INFN, P.O. Box 13, I-00044 Frascati, Italy  
and Dipartimento di Fisica, "E. Amaldi" Università di Roma Tre, Via della Vasca Navale 84, I-00146 Roma, Italy*

C. Raghu and D. D. Sarma

*Solid State and Structural Chemistry Unit, Indian Institute of Science, Bangalore 560 012, India  
(Received 17 January 1997)*

Ca-doped manganite  $\text{La}_{1-x}\text{Ca}_x\text{MnO}_3$  samples with  $x=0.2$  and  $0.4$  were investigated by extended x-ray absorption fine structure (EXAFS) as a function of temperature and preparation method. The samples exhibit characteristic resistivity change across the metal-insulator (MI) transition temperature whose shape and position depend on Ca-doping concentration and sample thermal treatment. EXAFS results evidenced an increase of nonthermal disorder at the MI transition temperature which is significantly correlated with the resistivity behavior. [S0163-1829(97)02732-X]

Hole-doped manganites of the general formula  $\text{Ln}_{1-x}\text{M}_x\text{MnO}_3$  where  $\text{Ln}$  is a lanthanide atom such as La or Pr and  $M$  represents a divalent metal ion such as Ca, Sr, Ba, or Pb have attracted a great deal of interest in the recent literature, leading to intense theoretical and experimental activities. The initial flurry of activities was triggered by the observation<sup>1</sup> of a pronounced negative magnetoresistance, now termed colossal magnetoresistance (CMR), in such materials which could have important technological implications. However, intense experimental activities have firmly established a more fundamental interest in these materials, as being unique in exhibiting a delicate balance and interplay between electronic, magnetic, and structural properties. On the theoretical side, qualitative understanding of the interrelationship between the electronic and magnetic degrees of freedom existed from very early works, starting with Zener,<sup>2</sup> who addressed the question of ferromagnetism in the hole-doped manganites. He pointed out that a strong *intra-atomic* exchange interaction (Hund's coupling) strength between the localized  $t_{2g}$  electrons and the delocalized conducting  $e_g$  electrons will lead to a ferromagnetic ground state related to the conductivity via the electron hopping from one Mn site to another; this mechanism, known as the double exchange, was put on a firmer theoretical basis by Anderson and Hasegawa,<sup>3</sup> de Gennes,<sup>4</sup> and Kubo and Ohata.<sup>5</sup>

At the beginning of recent activities on CMR materials, it was generally accepted that there is indeed a strong Hund's coupling strength between the localized  $t_{2g}$  and the conducting  $e_g$  electrons<sup>6</sup> and that Zener's double exchange mecha-

nism is fundamentally at the root of the unusual properties of these materials, inter-relating the electronic and magnetic properties. However, it also soon became clear that a pure double exchange mechanism does not account for many qualitative and quantitative aspects of the properties of these materials.<sup>7</sup> For example, it is not possible to explain the observed metal-insulator (MI) transition as a function of temperature in the hole-doped materials across the ferromagnetic transition temperature ( $T_c$ ).<sup>8</sup> Moreover, such a theory overestimated  $T_c$  by an order of magnitude.<sup>7</sup> Since the  $T_c$  in this model is related to the carrier concentration given directly by the dopant concentration  $x$ , it is easy to see that  $T_c$  can be markedly depressed if charge carrier concentration differs from dopant concentration as would be the case in the presence of lattice distortions trapping charge carriers locally. This has led to the inclusion of an electron-phonon interaction term in the usual double exchange Hamiltonian.<sup>9</sup> Results from this model exhibit several qualitative differences with respect to those obtained on the basis of only the double exchange mechanism and are in better agreement with the experimental observations. In particular,  $T_c$  is strongly reduced in the presence of the electron-phonon interactions. Moreover, a metal-insulator transition as a function of temperature appears due to a transition from a spatially homogeneous solution to a quasi-self-trapped state due to the formation of small polarons. These results bring forth the unique point of strong interplay between the electronic, magnetic, and lattice degrees of freedom.

Even before these theoretical considerations, there was widespread speculation concerning the role of the coupling

to the lattice in these materials. In fact, being in a  $d^4$  electron configuration, the  $Mn^{3+}$  in the parent manganite is a Jahn-Teller ion giving rise to distortion of the  $MnO_6$  octahedra in  $LaMnO_3$ .<sup>10</sup> Though early crystallographic works suggested that hole doping beyond  $x \geq 0.2$  wipes out the lattice distortions giving rise to cubic structures, it has been considered that dynamical Jahn-Teller effects may persist at even higher dopant concentrations, providing an effective means for electron-phonon coupling. Recently, direct evidence for lattice distortions, reflecting itself as increased disorder parameters, was obtained from extended x-ray absorption fine structure (EXAFS) studies;<sup>11,12</sup> this disorder appears to vanish in the low temperature metallic phase, but is prominent in the high temperature insulating phase. This is, however, not very surprising considering the basic chemistry of these compounds: the insulating states will necessarily have the doped holes localized at some Mn sites, giving rise to distinct  $Mn^{3+}$  and  $Mn^{4+}$  sites. The localized  $Mn^{3+}$  sites will continue to exhibit the Jahn-Teller distortion, thus exhibiting a static and nearly temperature independent disorder in the insulating state, which disappears in the delocalized metallic state.

In spite of all the progress made in understanding these materials, it appears that the presence of a well-defined electron-phonon interaction does not, however, explain all the experimental observations. For example,  $T_c$  calculated with reasonable values of electron-phonon interactions<sup>9</sup> is still higher than experimentally observed values by a factor of 4 or so, the lattice helping to reduce the  $T_c$  by only a factor of about 2; moreover, increasing the strength of the electron-phonon interactions in order to depress the  $T_c$  further, the calculated  $T_c$  decreases with increasing substitution for  $x \geq 0.2$  (Ref. 9) in contrast to the experimentally observed increase of  $T_c$  with  $x$  between 0.2 and 0.4. Besides, there is direct evidence of progressive removal of delocalized electron states at  $E_F$  with increasing temperature below  $T_c$ ,<sup>8,13</sup> suggesting a temperature dependent role of disorder even within the metallic state. Thus it appears that there is more than just a static disorder dictated by a single Jahn-Teller coupling dominating the physics of these systems.

To investigate the role played by disorder in modifying the unusual properties of these CMR materials in general and metal-insulator transitions in particular, we have reinvestigated the local structure around Mn ions in these systems as a function of temperature using the EXAFS technique. We have chosen the  $La_{1-x}Ca_xMnO_3$  system for this purpose, as the metal-insulator transition in this series has been well characterized in the literature. In these systems, the metal-insulator transition temperature can be systematically varied by changing  $x$ ; more interestingly, the transition temperature can be substantially modified even for a fixed  $x$  by varying the heat treatment leading to different particle sizes.<sup>14,15</sup> Thus we have produced two sets of samples with  $x=0.2$  and 0.4 in  $La_{1-x}Ca_xMnO_3$ . Sample set A is produced by heating the stoichiometric reaction mixtures at 1400 °C for 24 hours, producing typical grain sizes slightly below 1  $\mu m$ , while sample set B is obtained by further heating the set A at the same temperature but for another 48 hours, with particle sizes in the vicinity of 2–4  $\mu m$ . We also carried out EXAFS measurements on two reference samples,  $LaMnO_3$  and  $MnO$ . While  $LaMnO_3$  provides the reference point for systems with

disorder arising from static Jahn-Teller distortions at all temperatures,  $Mn^{2+}$  in  $MnO$  with a  $d^5$  electron configuration has no such substantial disorder and the disorder parameter in this case provides predominantly a typical phononlike dependence on the temperature.

We performed EXAFS measurements in the energy range 6.2–7.6 KeV at the Mn  $K$  edge in transmission geometry at the Italian CRG-GILDA beamline<sup>16</sup> at the European Synchrotron Radiation Facility (ESRF) in Grenoble using a Si(311) double crystal sagittal focusing monochromator.<sup>17</sup> The dynamical sagittal focusing ensured a stable beam size of about 2  $mm^2$  on the sample during each scan. Samples were mounted on a liquid nitrogen cryostat, monitoring the temperature with a thermocouple placed close to the samples. Great care was taken in the data analysis procedure following the suggestions of the International Workshop on Standard in XAFS.<sup>18</sup> EXAFS oscillations,  $\chi(k)$ , were extracted from the data using standard procedures;<sup>19</sup> normalization was performed using the Lengeler-Eisenberger method.<sup>20</sup> The  $\chi(k)$  data were Fourier transformed with  $k^3$  weight in the  $k$  range of 3–11  $\text{\AA}^{-1}$ . Mn-O first shell EXAFS oscillations were isolated by inverse Fourier filtering in the  $R$  range of 0.7–2.15  $\text{\AA}$ . Ca doping of  $LaMnO_3$  reduces the static Jahn-Teller distortion of  $Mn^{3+}$  octahedra and far from  $T_c$  all six Mn-O bond lengths are similar<sup>21</sup> despite the simultaneous presence of  $Mn^{3+}$  and  $Mn^{4+}$  ions. The distortion expected at  $T_c$  is of the order of 0.1  $\text{\AA}$ ;<sup>10,23</sup> at this level the EXAFS does not have enough resolution to separate the contributions which are seen as a single shell with an increased Debye-Waller factor. Therefore we employ a single shell model to fit the Fourier filtered data using the theoretical amplitudes and phases calculated by McKale.<sup>22</sup> The theoretical functions were tested on standard  $MnO$  and  $LaMnO_3$  samples, obtaining an excellent agreement.

Since the main structural effect at the MI transition is expected to be on the Debye-Waller factor ( $\sigma^2$ ), in fitting the data those parameters strongly correlated to  $\sigma^2$ , namely, the Mn-O coordination number  $N$  and the photoelectron mean free path  $\gamma(k)$ , were fixed.  $N$  was fixed to 6, as dictated by the perovskite structure. The mean free path  $\gamma(k)$  was determined from the model compounds  $MnO$  and  $LaMnO_3$ . In all samples based on  $LaMnO_3$ , the Mn-O distance obtained was  $R_{Mn-O} = 1.95 \pm 0.005 \text{\AA}$ , approximately constant with temperature and in agreement with the literature.<sup>10</sup>

In Fig. 1 we show the so obtained temperature dependence of  $\sigma^2$  in  $MnO$  and the undoped perovskite  $LaMnO_3$ . In both samples  $\sigma^2$  has a nonstructured monotonous behavior with  $T$ . The dashed line represents the best fit obtained on the basis of a correlated Debye model<sup>24</sup> plus a temperature independent static disorder,  $\sigma^2 = \sigma_s^2 + \sigma_D^2$  in each case. The Debye temperatures estimated from these experiments are about 400 and 700 K for  $MnO$  and  $LaMnO_3$ , respectively. It turns out that the component of the static disorder,  $\sigma_s^2$ , is much larger in  $LaMnO_3$  ( $\sim 8 \times 10^{-3} \text{\AA}^2$ ) compared to that in  $MnO$  ( $\sim 2.4 \times 10^{-3} \text{\AA}^2$ ), reflecting the presence of the static Jahn-Teller distortion in the former compound. This also explains the relative insensitivity of the total disorder parameter,  $\sigma^2$ , on the temperature in the case of  $LaMnO_3$  compared to that of  $MnO$ , since  $\sigma^2(LaMnO_3)$  is dominated by the static disorder relatively independent of the temperature.

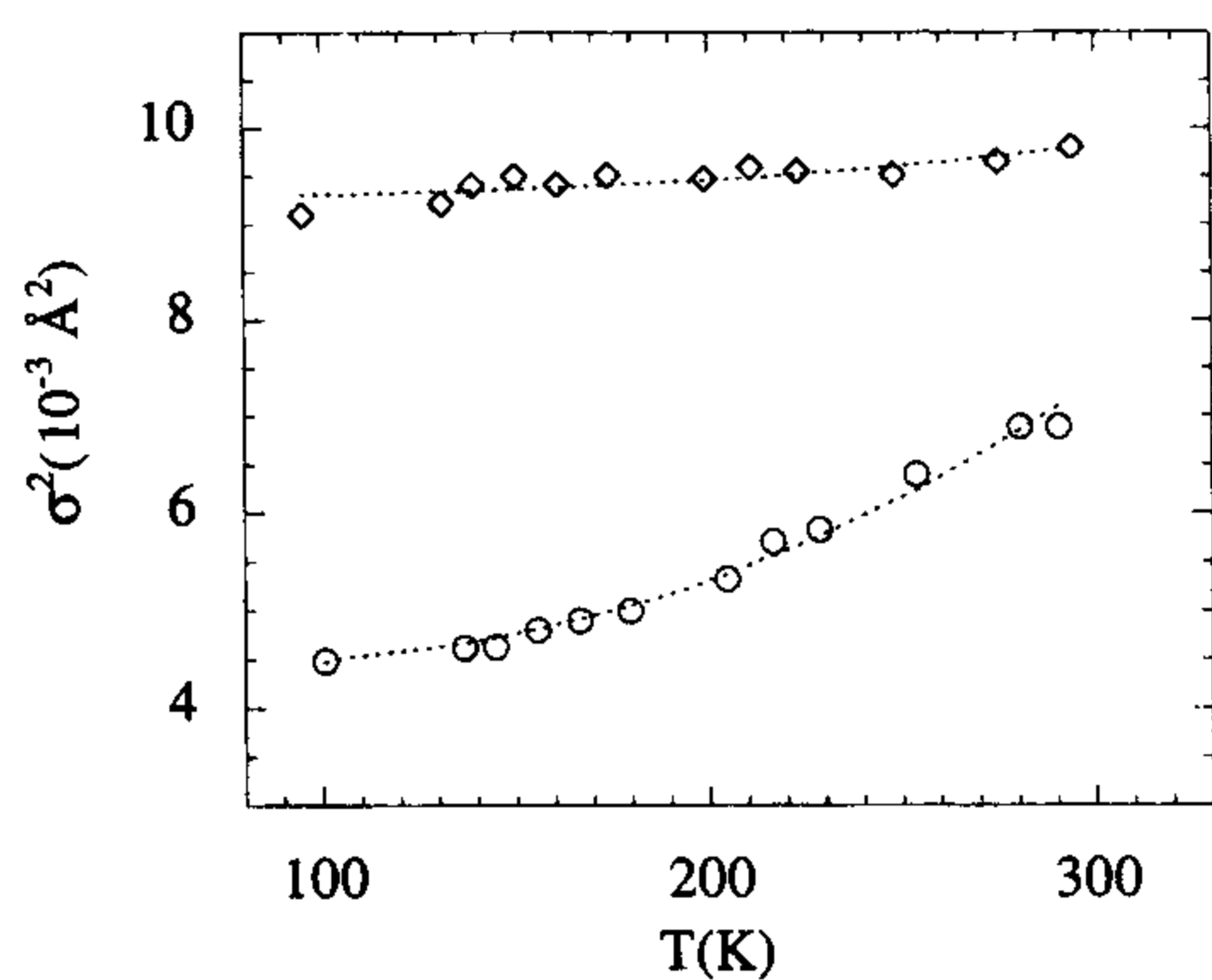


FIG. 1. Debye-Waller factor from EXAFS analysis for  $\text{LaMnO}_3$  (diamonds) and  $\text{MnO}$  (circles) samples. The dashed lines are the best fit data obtained using a correlated Debye model (see text).

In doped samples, the Debye-Waller factors exhibit more complex dependence on temperature. In the upper panels (a)–(d) of Fig. 2, we show the temperature dependence of  $\sigma^2$  in  $\text{La}_{1-x}\text{Ca}_x\text{MnO}_3$ ,  $x=0.2$  and  $0.4$ , samples A (small grain) and B (large grain), with the resistivities of the corresponding samples shown in the lower panels (e)–(h). Clearly, the variation of  $\sigma^2$  with  $T$  in any of the four cases is *qualitatively* different from those in Fig. 1, showing that a simple Debye-like or a Debye-plus-static disorder model does not explain the data. In all the doped samples the  $\sigma^2$  show evident slope changes near the MI transition temperatures indicated by arrows. To show the monotonic phonon and static contributions to  $\sigma^2$ , we fitted the data far from the MI transition temperature to a correlated Debye model (dashed curves in Fig. 2). The obtained fits have similar parameters with static contribution,  $\sigma_s^2$ , of  $\sim 4 \times 10^{-3}$  and

$\sim 3 \times 10^{-3} \text{ \AA}^2$  for  $x=0.2$  and  $0.4$  samples, respectively, irrespective of the grain size or the MI transition temperature. The Debye temperature was found to be about 380 K for all doped samples. This value is typical of doped perovskites and in good agreement with the literature data,<sup>25</sup> providing further credence to the present data analysis.

Comparing the experimental data and the fits, it is evident that there is a clear departure just in the region near the MI transition. This behavior appears to be unique to the doped samples showing the MI transition, while the undoped sample does not exhibit any such unusual behavior (see Fig. 1). A similar deviation in the peak heights in the pair distribution function analysis of neutron diffraction data<sup>23</sup> has been reported recently. In close analogy to the previous work, we interpret the unusual deviation of  $\sigma^2$  from the expected Debye-Waller behavior as an evidence for the formation of small polarons in the paramagnetic insulating phase giving rise to a distribution of Mn-O distances; interestingly our results also suggest the persistence of these polarons well into the ferromagnetic metallic state with decreasing temperature. These polarons disappear only at the lowest temperatures probed, recovering the Debye dependence of  $\sigma^2$ .

The residual part of the  $\sigma^2$ , which we define as the extra component of the disorder not explainable by the correlated Debye model plus a static disorder and suggesting the formation of lattice polarons, shows an unusual behavior in every case. It increases with lowering of temperature within the insulating phase, evidenced by the deviation from the calculated fits with decreasing  $T$ . Then it reaches a maximum exactly at the same temperature where the resistivity of the sample exhibits a maximum. This is followed by a steady decrease of the residual disorder within the metallic state. It is indeed interesting that the residual disorder parameter has

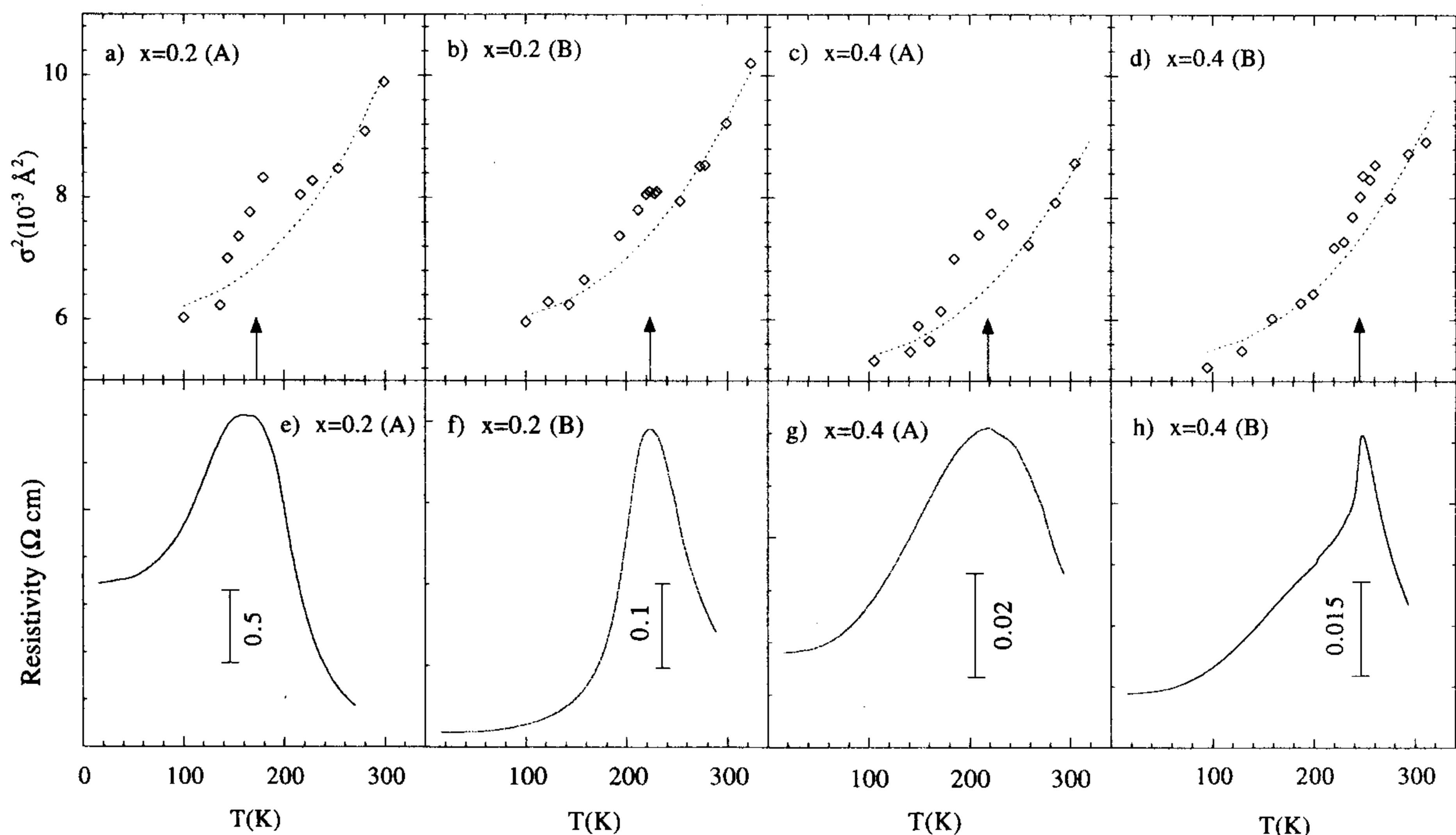


FIG. 2. Top panels (a)–(d): Debye-Waller disorder factor (diamonds) for Ca-doped  $\text{La}_{1-x}\text{MnO}_3\text{Ca}_x$  manganites. The arrows indicate the metal-insulator transition temperature and the dashed lines are the Debye-like contribution to the total disorder factor (see text). Bottom panels (e)–(h): resistivity data.

its maximum coincident with that of the resistivity in every case, even though this maximum for a fixed composition changes by as much as 50 K due to different heat treatments. This happens for both the compositions,  $x=0.2$  and  $0.4$ , firmly establishing the observation. More interestingly, the deviations of the disorder parameter,  $\sigma^2$ , from the expected fits (dashed lines in Fig. 2) appear to follow the overall shapes of the resistivity plots in every case. Thus we find that the residual disorder is spread over a wider temperature range for samples A with smaller grain size [Figs. 2(a) and 2(c)] and the corresponding resistivity plots [Figs. 2(e) and 2(g)] are also broad. This is in contrast to narrower distributions of both the residual disorder [Figs. 2(b) and 2(d)] and the resistivities [Figs. 2(f) and 2(h)] for samples with larger grain sizes, independent of the sample composition. Significantly, we also find a substantial amount of residual disorder in the metallic regime ( $T < T_m$ ), which gradually decreases with the decreasing temperature. This observation appears to be related to the unusual decrease of spectral weight at  $E_F$  with increasing temperature observed in these materials earlier.<sup>13,8</sup> Our observation of increasing disorder with increasing  $T$  in this regime would suggest that such disorder effects are concomitant with the formation of polaronic self-trapped states<sup>9</sup> removing delocalized charge carriers from the system and thus leading to a decreasing weight at  $E_F$ . The same effects are also likely to be responsible for the unexpected redistribution of spectral weight over an unusually large energy range observed in these systems.<sup>13</sup>

In conclusion, we have presented detailed analysis of  $\sigma^2$  for the Mn-O coordination shell from EXAFS data for MnO and  $\text{La}_{1-x}\text{Ca}_x\text{MnO}_3$  ( $x=0.0, 0.2, \text{ and } 0.4$ ). While the disorder parameter exhibits the expected Debye dependence on temperature for MnO and  $\text{LaMnO}_3$ , it is distinctly different for the doped samples. The residual disorder parameter values for the doped samples compared to the expected Debye behavior suggest a progressive formation of lattice polarons with decreasing temperature within the paramagnetic insulating phase with the maximum in this extra  $\sigma^2$  coinciding exactly with the MI transition temperature. This is true even for samples where the Ca doping is kept fixed, though  $T_c$  could be substantially varied by changing the heat treatment for sample preparation. In every case studied, the residual  $\sigma^2$  follows the resistivity behavior of the doped samples closely, establishing the profound influence of temperature dependent polaron formation on the unusual properties of these doped manganites. The present results also provide an explanation for the unexpected temperature dependent electronic structure in such samples observed recently by electron spectroscopies.

We are grateful to the technical staff of the Laboratori Nazionali di Frascati-INFN: F. Campolungo, V. Sciarra, L. Sangiorgio, and V. Tullio for support. The project GILDA was financed by the Italian institutions CNR, INFM, and INFN.

<sup>1</sup>R. von Helmolt *et al.*, Phys. Rev. Lett. **71**, 2331 (1993).

<sup>2</sup>C. Zener, Phys. Rev. **82**, 403 (1951).

<sup>3</sup>P. W. Anderson and H. Hasegawa, Phys. Rev. **100**, 675 (1955).

<sup>4</sup>P. G. deGennes, Phys. Rev. **118**, 141 (1960).

<sup>5</sup>K. Kubo and N. Ohata, J. Phys. Soc. Jpn. **33**, 21 (1972).

<sup>6</sup>D. D. Sarma *et al.*, Phys. Rev. Lett. **75**, 1126 (1995); S. Satpathy *et al.*, *ibid.* **76**, 960 (1996); Priya Mahadevan, N. Shanthi, and D. D. Sarma, J. Phys., Condens. Matter **9**, 3229 (1997).

<sup>7</sup>A. J. Millis, P. B. Littlewood, and B. I. Shraiman, Phys. Rev. Lett. **74**, 5144 (1995).

<sup>8</sup>J. H. Park *et al.*, Phys. Rev. Lett. **76**, 4215 (1996).

<sup>9</sup>H. Roder, Jun Zang, and A. R. Bishop, Phys. Rev. Lett. **76**, 1356 (1996).

<sup>10</sup>S. Satpathy, Z. S. Popović, and F. R. Vukajlović, Phys. Rev. Lett. **76**, 960 (1996).

<sup>11</sup>T. A. Tyson *et al.*, Phys. Rev. B **53**, 13 985 (1996).

<sup>12</sup>C. H. Booth *et al.*, Phys. Rev. B **54**, 15 606 (1996).

<sup>13</sup>D. D. Sarma *et al.*, Phys. Rev. B **53**, 6873 (1996).

<sup>14</sup>R. Mahesh *et al.*, Appl. Phys. Lett. **68**, 2291 (1996).

<sup>15</sup>M. F. Hundley *et al.*, J. Appl. Phys. **79**, 4535 (1996).

<sup>16</sup>S. Pascarelli *et al.*, ESRF Newsletter **23**, 17 (1995).

<sup>17</sup>S. Pascarelli *et al.*, J. Synchrotron Radiat. **3**, 147 (1996).

<sup>18</sup>F. W. Lytle, D. E. Sayers, and E. A. Stern, Physica B **158**, 701 (1989).

<sup>19</sup>P. A. Lee, P. H. Citrin, P. Eisenberger, and B. M. Kinkaid, Rev. Mod. Phys. **53**, 769 (1981).

<sup>20</sup>B. Lengeler and P. Eisenberger, Phys. Rev. B **21**, 4507 (1980).

<sup>21</sup>P. G. Radaelli *et al.*, Phys. Rev. Lett. **75**, 4488 (1995).

<sup>22</sup>A. G. McKale, J. Am. Chem. Soc. **110**, 3763 (1988).

<sup>23</sup>S. J. L. Billinge *et al.*, Phys. Rev. Lett. **77**, 715 (1996).

<sup>24</sup>G. Beni and P. M. Platzmann, Phys. Rev. B **14**, 9514 (1976).

<sup>25</sup>J. J. Hamilton *et al.*, Phys. Rev. B **54**, 14 926 (1996).